

Development of a Two Dimensional Position Sensitive Transition Radiation Detector for High Counting Rate Experiments

M. Petriș, M. Petrovici, V. Cătănescu

National Institute of Physics and Nuclear Engineering (IFIN-HH),
Bucharest-Magurele, P.O.Box MG-6, RO-077125, Romania

Abstract. The CBM experiment is a heavy ion fixed target experiment at the future accelerator FAIR, aiming to investigate the properties of nuclear matter at extreme conditions of temperature and baryonic density. Transition radiation detectors (TRD) for identification of high-momentum electrons with a pion rejection factor of 100 for 90% electron efficiency and tracking of all charged particles are considered to be part of the experimental set-up. The most forward CBM-TRD detectors have to cope with counting rates up to 100 kHz/cm². The TRD prototypes developed by our group fulfill the required performance for electron discrimination with a minimized number of TRD layers. They provide as well the position information across and along the readout electrode pads with a single TRD layer with very good position resolutions. The TRD prototypes were tested using a new front-end ASIC called Fast Analog Signal Processor (FASP) developed by us.

1 Introduction

The CBM (Compressed Baryonic Matter) experiment [1] at the future Facility for Antiproton and Ion Research (FAIR) in Darmstadt [2] is designed to measure hadrons, multi-strange hyperons, lepton pairs and charmed particles produced in nuclear collisions up to 10 MHz interaction rate with a large acceptance.

The CBM experimental set-up includes a transition radiation detector (TRD) for identification of high-momentum electrons. At the same time it will perform intermediate tracking in order to match tracks reconstructed in the silicon tracking system (STS) to the time-of-flight (TOF) system.

It should perform position reconstruction for all charged particles with a position resolution across the pads of 200–400 μm and 3–30 mm along the pads and electron identification with a pion efficiency better than 1% for 90% electron efficiency. Being a fixed target experiment, the most forward angles of CBM have to cope with a counting rate up to 100 kHz/cm² for 10⁷ interactions/s of minimum bias Au+Au collisions at 25 A·GeV [1]. Therefore a fast detector is required.

2 First Results Based on a High Counting Rate TRD Prototype

The design and construction of the first detector prototype was decided based on the existing large scale TRD systems used for tracking and electron identification: ALICE TRD [3] and ATLAS - Transition Radiation Tracker (TRT) [4]. They illustrate two complementary approaches: the ALICE - TRD is a multiwire proportional chamber with a high granularity readout electrode in order to maintain its performances up to the highest multiplicity anticipated in $\sqrt{s_{NN}} = 5.5$ TeV Pb-Pb collisions at the LHC. The Transition Radiation Tracker of the ATLAS experiment is based on straw tubes and fulfills the requirements of preserving its performances up to 20 MHz/(readout channel) counting rate, at moderate multiplicity per event in p-p collisions at $\sqrt{s} = 14$ TeV.

Therefore, the solution for a fast TRD detector with high granularity which can cope with the mentioned high counting rates was a Multiwire Proportional Chamber (MWPC) [5]. It was designed and built with a minimized drift region of 3 mm gas gap between the anode and the cathode planes, in order to reach the required speed of the readout of the signals and to reduce the possible space charge effects.

The prototype was tested first with an ^{55}Fe source [5] and in-beam at the SIS18 accelerator of GSI, Darmstadt. The effect of the high counting rate environment on the detector performance was studied using a mixture of positive particles of 2 GeV/c momentum, in which the protons have been the dominant component.

The effect of the space charge on the gas gain [6] can be seen in Figure 1a in terms of pulse height and in Figure 1b in terms of integrated charge. The relative degradation of the pulse height and of the integrated charge was $3.2\% \pm 2.1\%$ (Figure 1a) and $5.0\% \pm 3.4\%$ (Figure 1b), respectively, at the highest rate of 10^5 particles/(cm²·s), for a 85%Xe + 15%CO₂ gas mixture and 1800 V applied anode voltage.

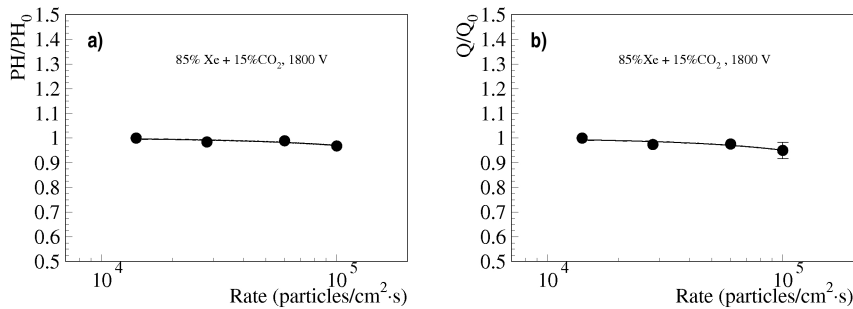


Figure 1. The rate dependence of the most probable value (mpv) normalized to the mpv value at the lowest rate of a) the pulse height distribution and b) the charge distribution, for a Xe/CO₂(15%) gas mixture at 1800 V applied voltage.

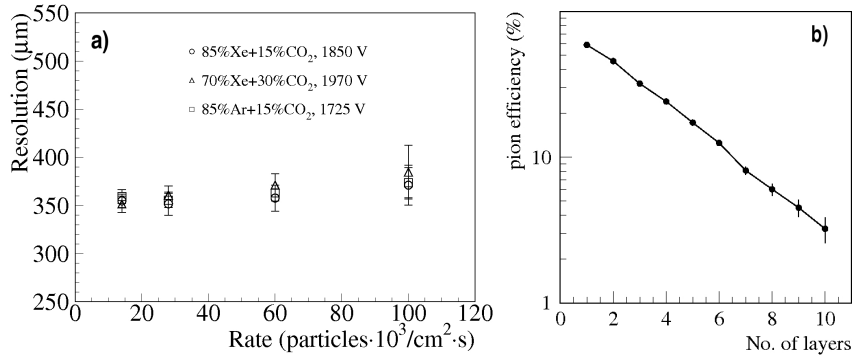


Figure 2. a) Position resolution as a function of the counting rate for different gas mixtures and applied voltages. b) Pion efficiency at 90% electron efficiency at 1 GeV/c momentum as a function of number of TRD layers for a Rohacell HF71 radiator and 1900 V anode voltage.

The position was reconstructed from the charge sharing among three neighbouring pads (p_{i-1} , p_i , p_{i+1}) along the anode wires. At the lowest rate the position resolution is $\sim 350 \mu\text{m}$ and its degradation as a function of rate is less than $40 \mu\text{m}$ (Figure 2b). One should mention that for this prototype the pad sizes, $7.5 \times 80.0 \text{ mm}^2$, were not optimized to reach the position resolution required by the CBM experiment.

It is well known that with a single TRD layer (radiator + chamber) the discrimination between electrons and pions is rather modest. A decisive factor in designing a large area TRD detector is the number of layers needed for a desired rejection power. The total number of readout channels, the total size of the detector and the total amount of material budget are related to this. The electron identification performance of a TRD is quantified in terms of pion efficiency (or pion misidentification probability) at a given electron efficiency and is the fraction of pions wrongly identified as electrons at a given electron efficiency. The obtained pion efficiency (Figure 2b) for a six layer configuration is 12.5% and of 2.9% for ten TRD layers, for a Xe based gas mixture with 15% CO₂ and 1900 V anode voltage, for 1 GeV/c particle momentum. Such efficiency could be reached with less layers (lower material budget, lower cost) using a regular periodic stack foil radiator instead of Rohacell HF71 [3]. The main reason for the large number of layers of such architecture is the low conversion efficiency of transition radiation (TR) in the thin gas layer.

3 Double-Sided High Counting Rate TRD Prototype

In order to maintain the counting rate performance and increase the conversion efficiency of the TR in a single layer, we designed and built an original TRD architecture for electron discrimination in a high counting rate environment [7].

It is based on two multiwire proportional chambers with a common double-sided pad structure read-out electrode, almost transparent to the TRs. Double-sided copper pad readout structure was etched on 25 μm kapton foil with the copper evaporated on it.

The configuration of this prototype is symmetric relative to the central read-out electrode which divides the detector in two identical halves and has identical pad structure (of 0.5×1 cm size each) on both sides. The corresponding pads on the upper and lower surface are electrically connected together. The anode-cathode gap and the anode wire pitch are kept the same as in the former prototype discussed in the previous chapter, i.e. 3 mm and 2.5 mm, respectively. The detector maintains the timing properties of a single MWPC [5] while the gas thickness for TR conversion is doubled. In this configuration a TR photon produced in a radiator by an incident high momentum electron can be absorbed either in the first MWPC or in the second MWPC after crossing the readout electrode with low TR absorption. Therefore, the conversion probability significantly increases relative to the single sided configuration.

The detector prototype was tested in the Hadron Physics Department detector laboratory with ^{55}Fe source [7] and with mixed secondary e/π beams at the SIS18 accelerator of GSI Darmstadt. A structure of fibres of about 4.0 cm thickness and Rohacell HF71 of 2.0 cm thickness [3] and a stack of 120 polypropylene foils of 20 μm thickness and 500 μm gap, (Reg1(20/500/120)) were used as radiators. The detector was operated with a xenon based gas mixture (85%Xe + 15%CO₂).

The pion efficiency was extracted using the likelihood on integrated energy deposit [9]. For an energy deposit E_i in layer i , $P(E_i|e)$ is the probability that it was produced by an electron and $P(E_i|\pi)$ is the probability that it was produced by a pion. The likelihood L , to be an electron, is:

$$L = P_e / (P_e + P_\pi), \quad (1)$$

where

$$P_e = \prod_{i=1}^N P(E_i | e); P_\pi = \prod_{i=1}^N P(E_i | \pi). \quad (2)$$

For a six layers configuration a pion efficiency of 3.32% at 90% electron efficiency for the Rohacell radiator, 1.5 GeV/c particle momentum and 1800 V anode voltage is reached (Figure 3, red squares). For the run with the regular radiator Reg1(20/500/120) the pion efficiency was of 1.1% at an anode voltage of 1700 V (Figure 3, blue circles). Using the Rohacell radiator, a pion efficiency of 5.43% was obtained (Figure 3, blue squares) at the same 1700 V anode voltage. As one could see, for six TRD layers, the Reg1(20/500/120) radiator improves the pion efficiency by a factor of 5. If one considers this improvement factor and apply it to the previous run (at 1800 V anode voltage), the extrapolated pion efficiency for a six layer stack and Reg1 foil radiator is 0.67%.

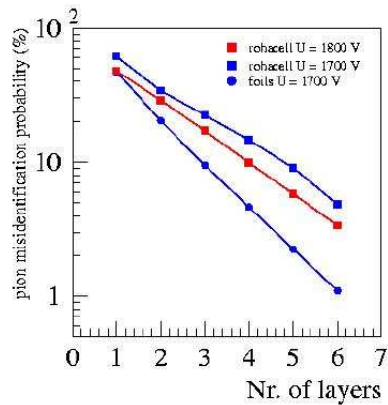


Figure 3. Pion efficiency at 90% electron efficiency at 1 GeV/c momentum as a function of number of TRD layers for a Rohacell HF71 radiator and two anode voltages, i.e. 1800 V (red squares) and 1700 V (blue squares) and regular foil radiator and 1700 V anode voltage (blue dots).

The effect of the high counting rate on the detector performance was tested using a mixture of positive particles of 1.5 GeV/c momentum in which the protons have been the main component.

The behaviour of the gain in terms of pulse height as a function of counting rate can be followed in Figure 4a and of the position resolution in Figure 4b. As one could see, up to counting rate of 250×10^3 particles/(s·cm²) no significant deterioration of the gas gain or position resolution is observed.

Figure 5 shows the pulse height distributions of pions and electrons, respectively, for 26×10^3 particles/(s·cm²), 65×10^3 particles/(s·cm²) and 110×10^3 particles/(s·cm²) counting rates. As far as the differences are within the experimental errors one could conclude that these detectors conserve also their pion efficiency performance up to $\sim 200 \times 10^3$ particles/(s·cm²) counting rate.

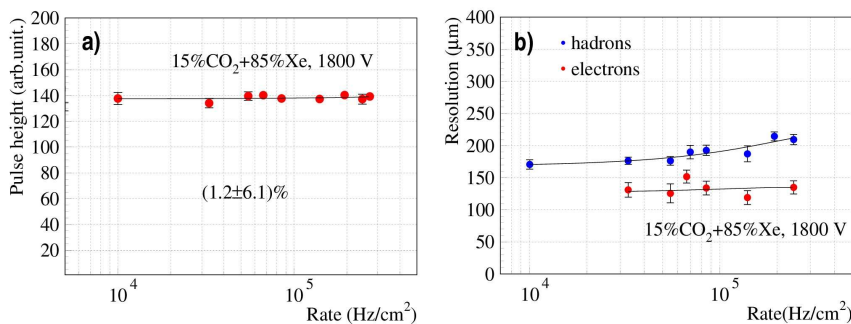


Figure 4. a) The most probable values of the Landau fit of the pulse height distribution as a function of counting rate. b) Position resolution as a function of counting rate.

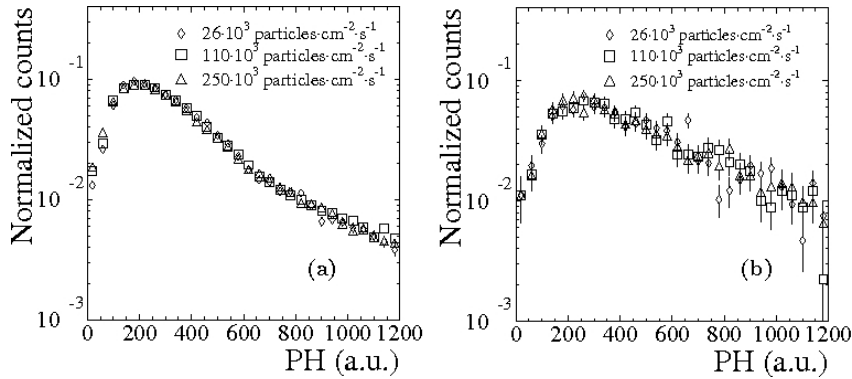


Figure 5. Pulse height distributions of: a) pions and b) electrons for 26×10^3 particles/(s cm²), 65×10^3 particles/(s cm²) and 110×10^3 particles/(s cm²) counting rates.

4 Two-Dimensional Position Sensitive TRD

With the aim to access the position information in both coordinates of the read-out electrode pad-plane (across and along the pads) with a single TRD layer, a new architecture for the readout electrode was designed. For the two-dimensional position sensitive TRD prototypes, the rectangular pads of the read-out electrode were split diagonally, each triangular pad being readout separately.

4.1 Two-dimensional position sensitive double-sided TRD and associated front-end electronics FASP

The prototype architecture [11] is similar with the previous described one: it is based on two MWPCs read out by a common double-sided central pad structure electrode [7, 12].

The readout electrode is made from a 25 μ m thickness kapton foil covered on both sides with evaporated Al/Cr (200 nm/20 nm) layers. It is almost “transparent” to the transition radiation (has a negligible absorption of about 1% for 5.9 keV X-ray of ⁵⁵Fe source). It has a row of 72 triangular pads along the anode wires. The corresponding pads on the opposite sides of the pad plane are electrically connected together and use a single readout channel. Each pad has a width of 10 mm and a height of 80 mm with a readout cell area of 4 cm². The choice on triangular-pad geometry readout electrode allows for position determination in both coordinates: across and along the pads, respectively.

Two versions of the prototype, with the same active area of 8×36 cm², were built and tested. The first version of the prototype (DSTRD-V1) was built with a 4×3 mm gain region. It has the same gas thickness like the small size double sided TRD prototype presented in the previous chapter. In order to improve the charge sharing between adjacent pads for better position reconstruction [12] and increase even further the conversion efficiency, the second version (DSTRD-V2)

was built with a 4 x 4 mm gain region.

For pad signal processing a new dedicated front-end electronics (FEE) called Fast Analog Signal Processor (FASP) [13] has been developed. The ASIC chip was designed in AMS CMOS 0.35 μm technology. Its main characteristics are a selectable shaping time of 20 ns or 40 ns and a 6.2 mV/fC conversion gain. For a 25 pF input capacitance, the equivalent noise charge is less than 980 electrons for 40 ns shaping time and less than 1170 electrons for 20 ns shaping time. The power consumption is about 11 mW/channel. Detailed electronic tests performed on the integrated FEE were reported in [14]. This first version of FASP has 8 analog channels, each with two types of outputs: a typical semi-Gaussian shape and a peak-sensing (called “flat top”). The “flat top” output was designed based on the results of the performed measurements in high counting rate environment which showed a better behaviour as a function of counting rate using pulse height information than the integrated charge of the signal. All channels have a self trigger capability with variable threshold. For the present measurements the FASP was set at 40 ns shaping time.

For the first tests the detectors were operated with the new FEE and flushed with 80%Ar+20%CO₂ gas mixture at atmospheric pressure. For the pad signals the ⁵⁵Fe source spectrum was recorded. The spectrum shows a peak-resolution of $\sigma_E/E = 10\%$ with a clear Ar escape peak positioned at about half of the total absorption peak [11] for both types of outputs.

The detectors were tested afterward with a mixed electron/pion beam of 1 - 5 GeV/c momenta at T10 beam line of the CERN PS accelerator [15]. The detectors were flushed with 80%Xe+20%CO₂ gas mixture at atmospheric pressure. Two regular foil radiators were used in the measurements: Reg1(20/500/120) and Reg2(20/250/220). DSTRD-V1 was operated at 1700 V with Reg2 while DSTRD-V2 was operated at 2000 V with Reg1 radiator.

The pion efficiency as a function of number of TRD layers (Figure 6) was ob-

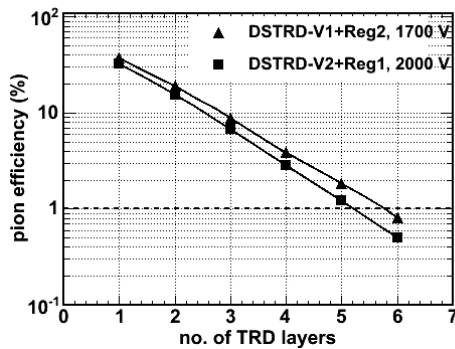


Figure 6. Pion efficiency as a function of number of TRD layers for 90% electron efficiency for DSTRD-V1+Reg2(20/250/220) – triangle and DSTRD-V2+Reg1(20/500/120) – rectangle

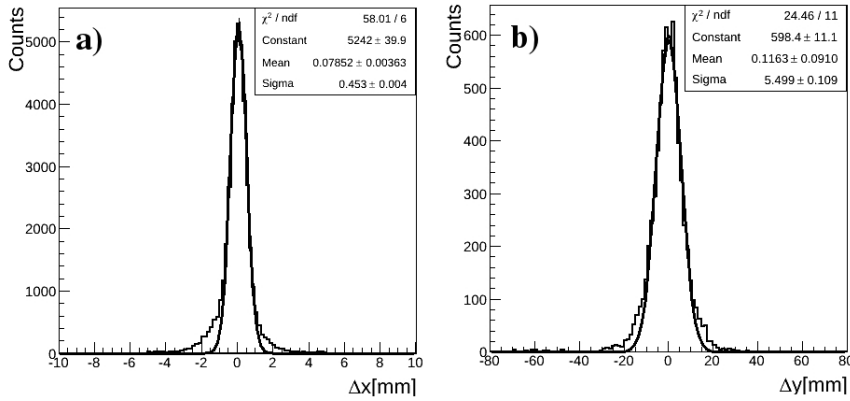


Figure 7. Distribution of the difference between the reconstructed position with the two prototypes fitted with a Gauss function: a) the x_{rec} coordinates, b) the y_{rec} coordinates

tained by Monte Carlo simulation taking as input the likelihood derived from the pulse height spectra. A pion efficiency of $(0.82 \pm 0.05)\%$ for a six layer configuration based on DSTRD-V1 is obtained. For a six layers configuration based on DSTRD-V2, the pion efficiency is improved by a factor of 1.6, i.e $(0.50 \pm 0.04)\%$. The errors are at the level of symbol size. The better pion suppression obtained with the second chamber is due to the thicker gas layer of DSTRD-V2 (4×4 mm) relative to DSTRD-V1 chamber (4×3 mm).

The position reconstruction across the pads was made using the signals induced on clusters of two or three rectangular pads [16]. For the position reconstruction along the pads, the algorithm described in [11] was followed. In order to estimate the position resolution, we used the position information from both detectors. With the assumption that the two prototypes have equal contribution, a position resolution across the pads of $320 \pm 4 \mu\text{m}$ (3.2% of the pad width) was obtained (Figure 7a). A 5.5 ± 0.11 mm (6.9% of the pad length) position resolution (Figure 7b) along the pads (y coordinate) was obtained.

4.2 Two-dimensional position sensitive single-sided transition radiation detector

Although it has a very good e/π discrimination in high-counting-rate environment, the size of the double-sided TRD (based on two MWPCs read out by a common double-side pad structure electrode) is limited by the topology of the signal extraction in the same plane as the readout electrode. For this reason, the geometrical efficiency of a large area TRD detector based on such an architecture is $<80\%$ for a single layer.

In order to overcome this problem we proposed a standard TRD architecture [17] of 2×4 mm amplification region coupled with a 4 mm drift zone (Single-Sided Transition Radiation Detector – SSTRD). It has a gas thickness identical to the 4×3 mm double-sided TRD prototype. The size of the drift

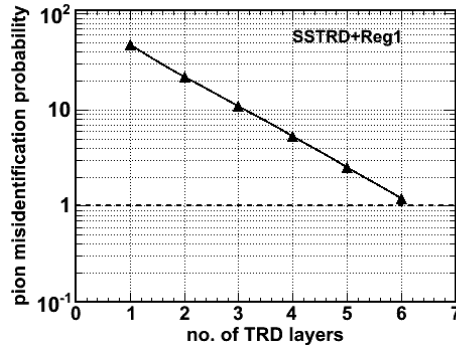


Figure 8. Pion misidentification probability as a function of number of TRD layers for 90% electron efficiency (the errors are at the level of symbol size)

zone was appropriately chosen to minimize the drift time of the ionization clusters inside the active volume, while keeping the TR conversion efficiency as large as possible.

The detector prototype was tested in the same in-beam measurement campaign as the prototypes described in the previous section.

An extrapolated pion misidentification probability of $(1.18 \pm 0.07)\%$ for a six layer configuration based on this architecture (Figure 8) was obtained. This SSTRD chamber has the same gas thickness for TR absorption as the double-sided architecture with 3 mm anode-cathode distance for which a pion efficiency of 0.8% was obtained. The difference could be explained in the case of latest prototype with a drift zone, by the large drift time difference for some ionization clusters, FASP with a 40 ns shaping time not being able to integrate them. A new FASP version with a 100 ns shaping time and many other interesting features implemented was designed and submitted for production.

5 Conclusions

The high counting rate performance of the TRD prototypes were demonstrated exposing the detectors on a surface equal with the beam size. They must be completed with high counting rate tests on the whole active area of the detectors.

Double sided architecture of 4×4 mm gas thickness has the highest electron/pion discrimination performance operated with FASP with 40 ns shaping time. However, geometric efficiency of a large TRD detector based on such an architecture is $< 80\%$ for a single layer.

Single sided architecture with 2×4 mm + 4 mm gas thickness operated with FASP with 40 ns shaping time has still a good discrimination performance of $\sim 1\%$ pion misidentification probability; geometric efficiency of a large TRD detector based on such an architecture is $> 90\%$ for a single TRD layer.

Triangular pad geometry of the readout electrode gives access to two dimen-

sional position reconstruction with good position resolution with a single TRD layer.

FASP can be considered as optimum FEE in terms of performance and amount of information to be processed and stored. A new FASP version with 100 ns shaping time and different internal pairing of triangular pads was designed and is currently in production.

Acknowledgements

We acknowledge V. Aprodu, D. Bartoş, I. Berceanu, A. Bercuci, G. Caragheorghopol, F. Constantin, V. Duţă, L. Prodan, A. Radu, L. Rădulescu, V. Simion, M. Târziă for their essential contribution to the reported results. This work was supported by EU-FP7/HP3-WP19 grant no.283286, NASR/CAPACITATI 179EU Project, RO-FAIR Project and NASR/NUCLEU Project

References

- [1] CBM Collaboration, “Compressed Baryonic Matter Experiment, Technical Status Report”, GSI Darmstadt, January 2005; URL: https://www-alt.gsi.de/documents/QCD_CBM-report-2005-001.html
- [2] URL: <http://www.fair-center.eu>
- [3] CERN/LHCC 2001-021, ALICE TRD 9 - TDR, 2001.
- [4] ATLAS, IDTDR, v.2, CERN/LHCC/97-17.
- [5] M. Petriş et al., *Nucl. Instr. and Meth. in Phys. Res. A* **581** (2007) 406
- [6] F. Sauli, “Principles of operation of multiwire proportional and drift chambers”, CERN 77-09, (1977).
- [7] M. Petrovici et al., *Nucl. Instr. and Meth. in Phys. Res. A* **579** (2007) 961
- [8] M. Klein-Bösing et al., *Nucl. Instr. and Meth. in Phys. Res. A* **585** (2008) 83
- [9] A.Büngener et al., *Nucl. Instr. and Meth. in Phys. Res. A* **214** (1983) 261
- [10] M. Petriş et al., *Rom. Journ. Phys.*, **55**, No.3-4 (2010), 32
- [11] M. Petriş et al., *Nucl. Instr. and Meth. in Phys. Res. A* **714** (2013) 17
- [12] M. Petrovici et al., *Rom. Journ. Phys.* **56**(2011) 654
- [13] V. Cătănescu et al., “CBM Progress Report 2009”, 47 ISBN 978-3-9811298-7-8, GSI Darmstadt, 2010
- [14] A. Caragheorghopol et al., “CBM Progress Report 2010”, 46 ISBN 978-3-9811298-8-5, GSI Darmstadt, 2011
- [15] D. Emschermann, C. Bergmann, “CBM Progress Report 2010”, 42 ISBN 978-3-9811298-8-5, GSI Darmstadt, 2011
- [16] W. Blum, W. Riegler, L. Rolandi, *Particle Detection with Drift Chambers*, Springer, Berlin, Heidelberg 2008
- [17] M. Petriş et al., *Nucl. Instr. and Meth. in Phys. Res. A* **732** (2013) 375